Finite volume method solution of pollutant transport in catchment sheet flow

Gokmen Tayfur, Zhiguo He and Qihua Ran

ABSTRACT

A finite volume numerical method was employed in the solution of two-dimensional pollutant transport in catchment sheet flow. The full dynamic wave constituted the sheet flow while the advection–diffusion equation with sink/source terms was the pollutant transport model. It is assumed that the solute in the surface active layer is uniformly distributed and the exchange rate of the solute between the active layer and overland flow are proportional to the difference between the concentrations in soil and water volume. Decrease of the solute transfer rate in the active surface layer caused by the transfer of solutes from soil to the overlying runoff is assumed to follow an exponential law. The equations governing sheet flow and pollutant transport are discretized using the finite volume method in space and an implicit backward difference scheme in time. The model was subjected to several numerical tests involving varying microtopographic surface, roughness, and infiltration. The results revealed that spatially varying microtopography plays an important role unlike the roughness and infiltration with respect to the total pollutant rate from the outlet of a catchment.

Key words | catchment, dynamic wave, finite volume, pollutant transport, sheet flow

Gokmen Tayfur (corresponding author)
Department of Civil Engineering,
Izmir Institute of Technology,
Urla,
Izmir,
Turkey
E-mail: *gokmentayfur@iyte.edu.tr*

Zhiguo He
Ocean College,
Zhejiang University,
Hangzhou 310058,
China

Qihua Ran
Department of Hydraulic and Ocean Engineering,
Zhejiang University,
Hangzhou 310058,
China

INTRODUCTION

Thousands of man-made chemicals, including fertilizers, pesticides, solvents, paint, petroleum by-products, and polychlorinated biphenyls, have contaminated the environment. Heavy metals, such as mercury, molybdenum, cadmium, and arsenic are also released in chemically active forms as a result of human activities. Man-made chemicals enter surface waters through aerial drift, run-off, or boating. Groundwater is contaminated by water leaching through soils – from stream flow or from direct sources, such as leaky petrol tanks or waste disposal sites.

Surface applied or soil incorporated pesticides, nutrients, and other agricultural chemicals are often transferred from the soil to surface runoff water during periods of heavy rainfall and surface irrigation. The transfer into runoff water decreases the efficiency of the applied chemical and poses a potential threat to the quality of the environment. Once released to runoff water, the chemicals can reach nearby surface water bodies, such as rivers, ponds, lakes, and reservoirs. Dissolved chemical in ponds and lakes may also indirectly reach groundwater (Wallach *et al.* 2001).

Overland flow is shallow and flow depth is in the order of cm (or even mm) and has low velocities, as compared to river flow (Tayfur & Kavvas 1998). Yet, it is the main cause of flash floods and, consequently, the water quality of rivers and lakes. According to Deng *et al.* (2005), storm runoff is one of the leading threats to water quality. It may contain a broad range of pollutants, among which are: (1) nutrients from fertilized lawns and roadsides; (2) bacteria from leaking sewers and septic tanks; (3) oil and grease from leaky motor vehicles, industrial areas, and illegal dumping; (4) heavy metals from vehicle wear and tear, vehicle exhausts, industrial areas; (5) toxic and synthetic chemicals from pesticide application. The highest concentration of these contaminants is often likely to be found in the first flush which delivers a large load of pollutants during the early part of the storm runoff event (Deng *et al.* 2005). This is because

doi: 10.2166/nh.2013.177

the stored pollutants that have accumulated on surfaces in dry weather quickly wash off at the beginning of a storm.

The process of soil-dissolved chemical transfer to runoff and its transport to the catchment outlet is complex. Modeling a large number of processes is involved and their interactions require the solution of relatively complicated, coupled linear, and nonlinear partial differential equations subject to time-dependent boundary conditions (Wallach *et al.* 2001). As a result, researchers have tended to simplify the process as one-dimensional (Peyton & Sanders 1990; Yan & Kahawita 2000; Walton *et al.* 2000; Wallach *et al.* 2001; Abbasi *et al.* 2003; Deng *et al.* 2005; Gitis *et al.* 2007 among others). Yan & Kahawita (2007) modeled solute transport in two dimensions and tested their model against their laboratory experiments.

In these modeling studies, unlike the natural catchment surface, the plane is often assumed as smooth with constant characteristics. Tayfur *et al.* (1993) and Tayfur & Singh (2004), modeling flow and sediment transport over the varying microtopographic surface of the experimental plot (given in Figure 1), showed that local physical variations drastically affect the flow depths, velocities, and sediment concentrations. Hence, this fact naturally implies that pollutant concentrations may also be affected under varying surface conditions. The objective of this study was to numerically investigate the effects of nonconstant characteristics of a catchment surface on pollutant transport.

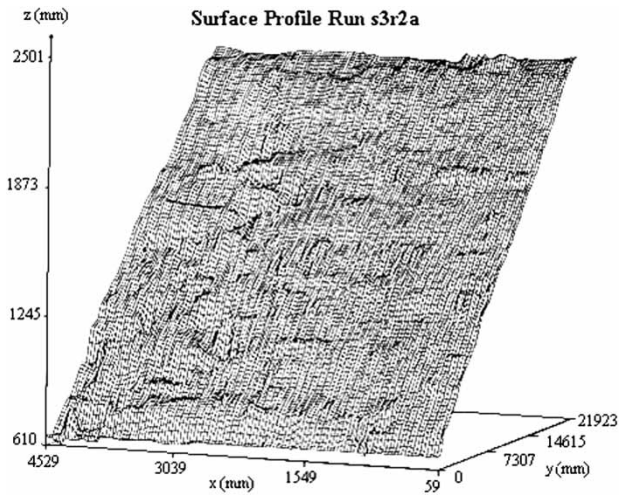

Figure 1 | Microtopographic surface of experimental plot S3R2A (Tayfur & Singh 2004).

MATHEMATICAL MODEL

Sheet flow model

Two-dimensional sheet flow equations can be expressed as follows (Tayfur *et al.* 1993; He *et al.* 2009):

$$\frac{\partial U}{\partial t}+\frac{\partial F}{\partial x}+\frac{\partial G}{\partial y}=S \tag{1}$$

where

$$U=\begin{bmatrix} h \\ hu \\ hv \end{bmatrix} \tag{2}$$

$$F=\begin{bmatrix} hu \\ huu \\ huv \end{bmatrix} \tag{3}$$

$$G=\begin{bmatrix} hv \\ huv \\ hvv \end{bmatrix} \tag{4}$$

$$S=\begin{bmatrix} r-i \\ -gh\dfrac{\partial Z}{\partial x}-g\dfrac{n^2u\sqrt{u^2+v^2}}{h^{1/3}} \\ -gh\dfrac{\partial Z}{\partial x}-g\dfrac{n^2u\sqrt{u^2+v^2}}{h^{1/3}} \end{bmatrix} \tag{5}$$

where h is overland flow depth (L); r is rainfall intensity (L/T); i is infiltration rate (L/T); n is Manning's roughness coefficient ($L^{1/3}/T$); and u and v are flow velocities in the x- and y-directions, respectively (Figure 2). At the upstream boundary there is no flow entering the system. Zero-flow depth gradient and zero-flow velocity gradient in the x- and y-directions at the downstream end of the catchment are assumed.

Pollutant transport model

Pollutant transport in two-dimensional sheet flow can be expressed as follows (Govindaraju 1996):

$$\frac{\partial(ch)}{\partial t}+\frac{\partial(cuh)}{\partial x}+\frac{\partial(cvh)}{\partial y}=RD_m(c_s-c)+J_c+q_{co} \tag{6}$$

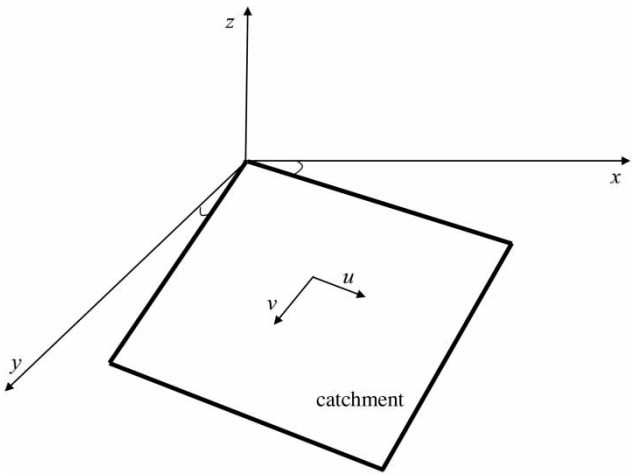

Figure 2 | Definition sketch for two-dimensional catchment flow.

where c is pollutant concentration in overland flow; c_s represents solute concentration in the active surface layer with a thickness of $D_m = \varepsilon h$, with h being the overland flow depth and ε being a dimensionless coefficient; R is exchange rate of solute between the active surface layer and the overlying flow; J_c is flux across the water surface per unit surface area; q_{co} is other source or sink term. u and v are flow velocities in x- and y-directions, respectively (Figure 2) and they are computed from the solution of Equations (1)–(5).

Equation (6) assumes that the pollutant in the uppermost active layer of soil is uniformly distributed and the exchange rate of pollutant between the active layer and sheet flow is proportional to the difference between concentrations in soil and water phases (Deng *et al.* 2005). Furthermore, since for overland pollutant transport, the diffusion term is generally negligible as compared to other terms (Abbott & Refsgaard 1996; Wallach *et al.* 2001), Equation (6) does not consider it.

Depletion of pollutant transfer rate in the active surface layer is assumed to follow an exponential law with a time constant μ as follows (Deng *et al.* 2005):

$$c_s = c_0 \exp(-\mu t) \tag{7}$$

where c_0 is initial pollutant concentration in the active layer. It is assumed that there is no pollutant entry from the upstream side. It is also assumed that zero-gradient pollutant concentration exits at the downstream side of the catchment. Equations (1) and (6) are solved simultaneously. Equation (1) is first solved to obtain spatial variation of flow depth and flow velocities (and flow discharges). Then, Equation (6) is solved to obtain pollutant concentrations (and pollutant rates) at the outlet of the catchment.

NUMERICAL SCHEME

The governing Equations (1) and (6) can be rewritten in the following general form:

$$\frac{\partial \Phi}{\partial t} + \frac{\partial}{\partial x}(u\Phi) + \frac{\partial}{\partial y}(v\Phi) = S_{c\Phi} \tag{8}$$

where Φ represents h and ch for the surface flow equation and pollutant transport equation, respectively; and $S_{c\Phi}$ includes all source terms in the equation for Φ.

Equation (8) is solved using the finite volume method which represents and evaluates partial differential equations in the form of algebraic equations. Similar to the finite difference method (or finite element method), the values are calculated at discrete places on a meshed geometry. 'Finite volume' refers to the small volume surrounding each node point on a mesh. In the finite volume method, volume integrals in a partial differential equation that contain a divergence term are converted to surface integrals, using the divergence theorem. These terms are then evaluated as fluxes at the surfaces of each finite volume. Because the flux entering a given volume is identical to that leaving the adjacent volume, these methods are conservative. Another advantage of the finite volume method is that it is easily formulated to allow for unstructured meshes. The method is used in many computational fluid dynamics packages.

The equations governing sheet flow and pollutant transport are discretized using the finite volume method in space and an implicit scheme in time. In the rectangular two-dimensional control volume, the discretized flow and pollutant transport equations can be expressed as follows:

$$\frac{\Phi_{i,j}^{t+1} - \Phi_{i,j}^{t}}{\Delta t} = -\left[(u\Phi)_{i+1/2,j}^{t+1} - (u\Phi)_{i-1/2,j}^{t+1}\right]/\Delta x_{i,j} - \left[(v\Phi)_{i,j+1/2}^{t+1} - (v\Phi)_{i,j+1/2}^{t+1}\right]/\Delta y_{i,j} + S_{c\Phi}. \tag{9}$$

Table 1 | Experimental conditions

Flume slope (–)	Rainfall intensity (mm/h)	Rainfall excess (mm/h)	Infiltration capacity (mm/h)	Rainfall duration (min)	Flow discharge (L/s)	Amount of pollutant (g/m^2)	Hydraulic conductivity (m/s)
10%	263.2	215.6	47.6	17.3	0.055	222.2	5.7×10^{-5}

Picard iterative technique was applied to handle the resulting nonlinear equations (He *et al.* 2009). The discretized equations were solved by the strongly implicit procedure (SIP) of Stone (1968). Accurate numerical solution and mass balance are reached when the convergence criteria of both the Picard iteration and SIP solution loops are satisfied at each time step. The operator Ψ, which is the nonlinear function of the surface roughness and friction slope, is evaluated as a cell parameter at the previous iteration as:

$$\Psi_P^{t+1,m+1} = \mathrm{Max}\left\{\varepsilon_m, \Psi_P^{t+1,m}\right\} \tag{10}$$

where ε_m is a small number (e.g., 10^{-8} to 10^{-10}) that, in the event of a zero fluid potential gradient, avoids a division by zero in Equation (10) by enforcing a minimum value of Ψ (Vander & Kwaak 1999).

In the discretized surface equation, variables at the control volume interface are evaluated by an upstream scheme, which ensures the solution monotonicity. The fluxes in Equation (10) are functions of the water depth and velocities and are determined by the operator ψ.

MODEL APPLICATION

Experimental data

The developed model was tested using an experimental study that investigated overland flow and associated pollutant transport over the soil surface during rainstorms (Deng *et al.* 2005). The experiment was carried out using a rainfall simulator and a soil flume with a dimension of 3.0 m length × 0.3 m width × 0.12 m height. Before running the experiments with a constant rainfall rate, the soil was wet to field capacity and 0.2 kg of granular salt with a mean diameter of 0.4 mm was applied uniformly onto the soil surface. The saturated water content is 39%, and the initial water content is 20%. During the experiments, surface runoff with pollutant was collected at the end of the flume, and then discharge, salt concentration, and pollutant transport rate were measured. The experimental conditions can be found in Table 1. The characteristics of soil and rainfall simulator are given in de Lima *et al.* (2003) and details of the experiment can be obtained from Deng *et al.* (2005).

To simulate the experiment, the developed model employed a mesh size of 22 × 22. The parameters used in the simulation, which were calibrated by Deng *et al.* (2005), are listed in Table 2. Figures 3 and 4 show that the numerical model predicts measured flow and pollutant rates satisfactorily with less than 5% error.

Numerical tests

To investigate the effects of spatially varying microtopographic surface, roughness, and infiltration rate on

Table 2 | Parameters used in the simulations

Roughness n	E (1/s)	μ (1/s)	c_0 (g/s)
0.025	0.04	0.022	3.68

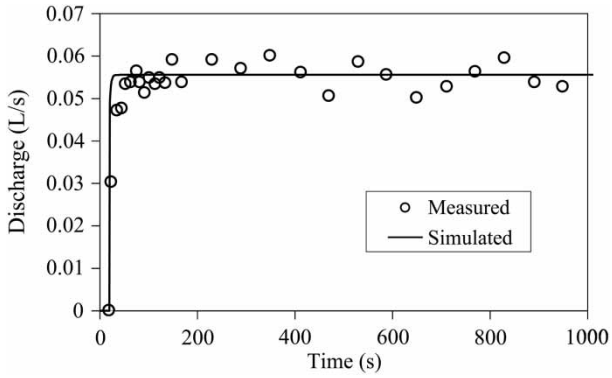

Figure 3 | Comparison between measured and simulated hydrographs.

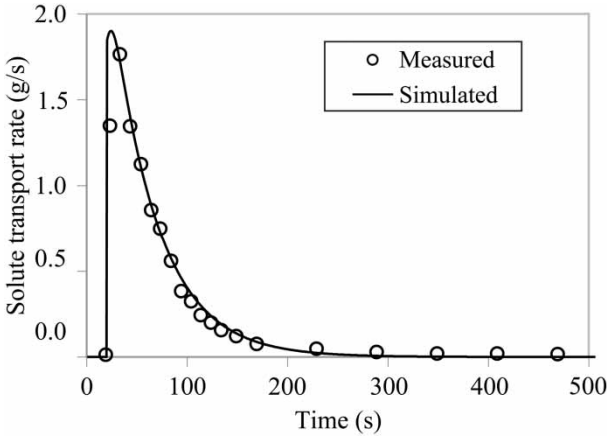

Figure 4 | Comparison between measured and simulated solute transport rates.

pollutant, a set of hypothetical data for spatially varying microtopographic surface, roughness, and infiltration rate were generated. The model simulated the overland flow and pollutant transport over a soil plot with a dimension of 3 m length × 3 m width, a constant slope of 10%, a Manning's roughness coefficient of 0.025, and a constant infiltration rate of 47.6 mm/h as a base case.

The hypothetical spatially varying microtopographic surface was generated over the 3 m × 3 m plot according to the random distribution function with a mean of 0.12 and a standard deviation of 0.03 (Figure 5). The range of the generated slope data was 0.04–0.16. The hypothetical spatially varying surface roughness was generated over the same plot according to the random distribution function with a mean of 0.025 and a standard deviation of 0.009 (Figure 6). The range of the generated data was 0.010–0.042, corresponding to bare sand (n: 0.010 to 0.016), gravel surface (n: 0.012 to 0.030), bare clay-loam soil (n: 0.012 to 0.033), and soil with grass (n: 0.03 to 0.05), which is physically sound. The hypothetical spatially varying infiltration rate was generated over the plot according to the random distribution function with a mean of 44 mm/h and a standard deviation of 20 mm/h (Figure 7). The range of the generated data was 5–90 mm/h, corresponding to loam (I: 3.4 mm/h), silt loam (I: 6.5 mm/h), sandy loam (I: 11 mm/h), loamy sand (I: 30 mm/h), and fine sand (I: 100 mm/h), which is physically sound. One may generate many different random fields of microtopographic surface, surface roughness, and infiltration rate with the same mean and

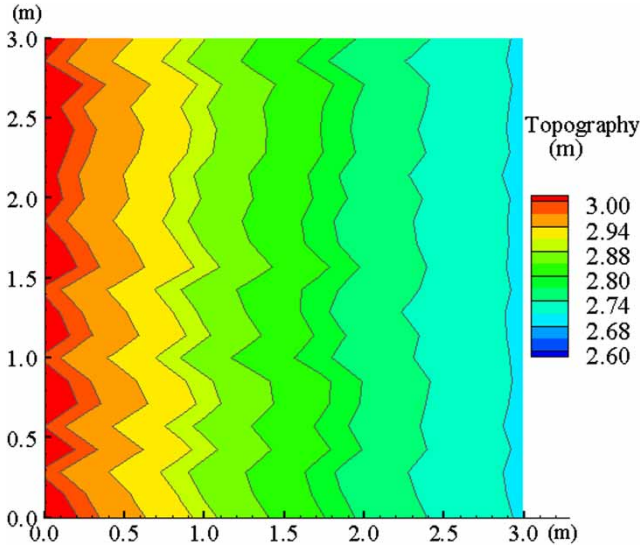

Figure 5 | Spatial distribution of microtopographic surface.

standard deviation. However, to have an insight into the effects of employing varying parameters, as opposed to constant average values, on the pollutant concentration profile, employing a single realization may be sufficient (Tayfur & Singh 2004), as is done in this study.

Figure 8 shows velocity, streamline, and depth while Figure 9 presents pollutant rate distribution under the spatially varying microtopographic surface, at a simulation time equal to 130 s when runoff reaches equilibrium. As seen in Figure 9, pollutant transport rates have a

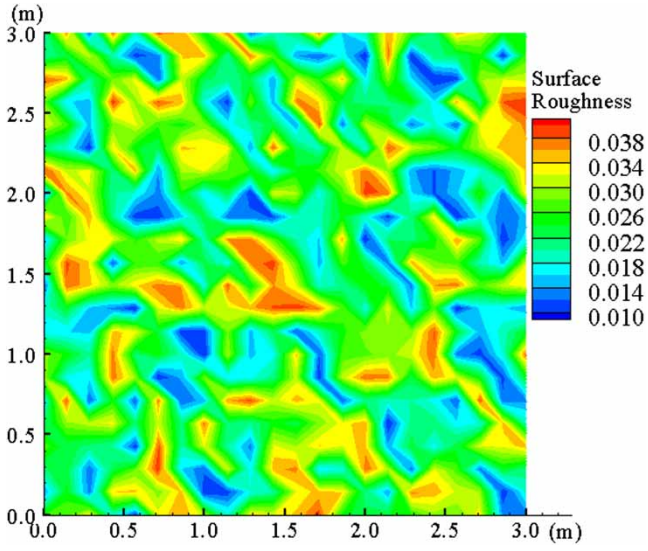

Figure 6 | Spatial distribution of surface roughness.

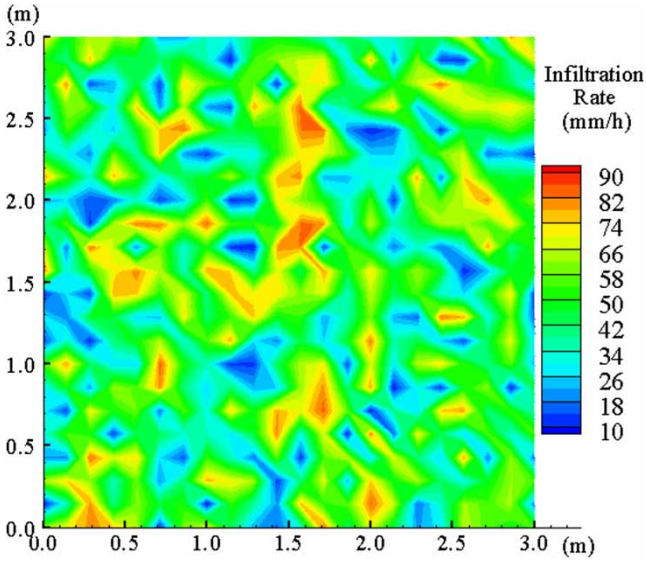

Figure 7 | Spatial distribution of infiltration rate.

non-smooth profile, clearly reflecting the impact of the spatially varying slopes which influence the flow depth, velocity, and flow path, as shown in Figure 8. Figure 10 presents transport rates using three sets of variable slopes, different spatially but with the same mean and standard deviation and constant slopes. As can be seen, the variable slopes with different spatial values do not significantly influence the results when they have the same mean and standard deviation. The employment of average constant slopes overestimated the pollutant rate by about 10%.

Figures 11 and 12 show water depth and pollutant rate under the spatially varying surface roughness, at the simulation time of 130 s. The variable roughness has less impact on pollutant transport than varying slopes. The rates in the upstream are generally lower than those in the

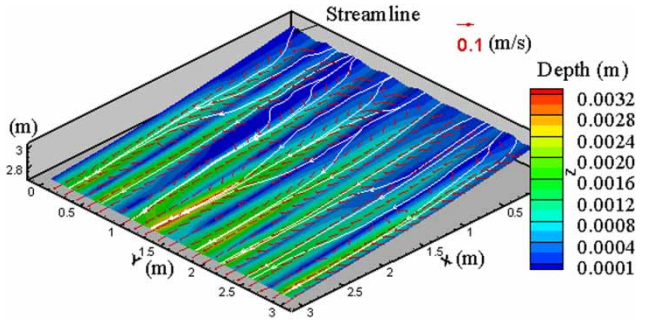

Figure 8 | Water depth, velocity, and streamline under the spatially varying microtopographic surface.

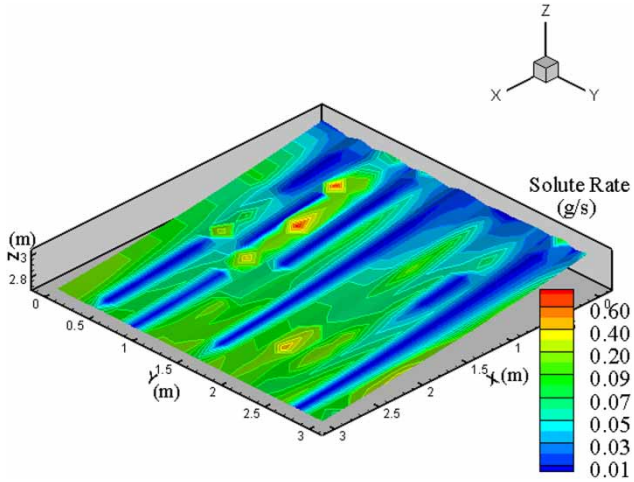

Figure 9 | Pollutant rate under the spatially varying microtopographic surface.

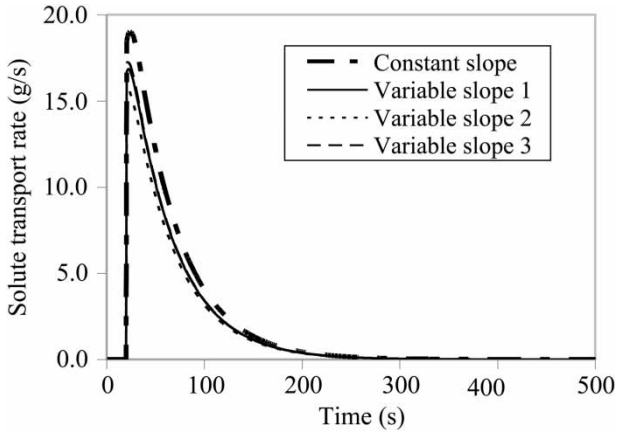

Figure 10 | Comparison of pollutant transport rate under constant (12%) and variable surface slope (mean is 0.12 and standard deviation is 0.03).

downstream (Figure 12). Figure 13 compares the pollutant transport rates and concentrations under constant and three different variable surface roughnesses. As is seen, an insignificant influence is observed on pollutant rate under global roughness and varying roughness cases.

Figures 14 and 15 show water depth and pollutant rate under the spatially varying infiltration rate, at the simulation time of 130 s. Similar to the variable roughness case, the variable infiltration rate has less impact on transport rate profiles (Figure 15). Figure 16 compares pollutant transport rates under constant and three variable infiltration rates, different in spatial but with the same mean and standard deviation. As seen, replacing varying infiltration rates with

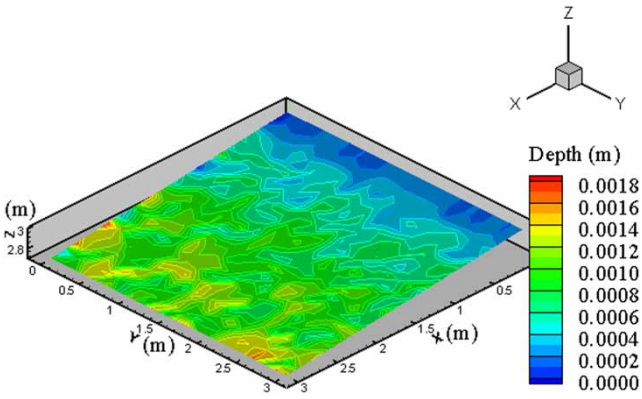

Figure 11 | Water depth under the spatially varying surface roughness.

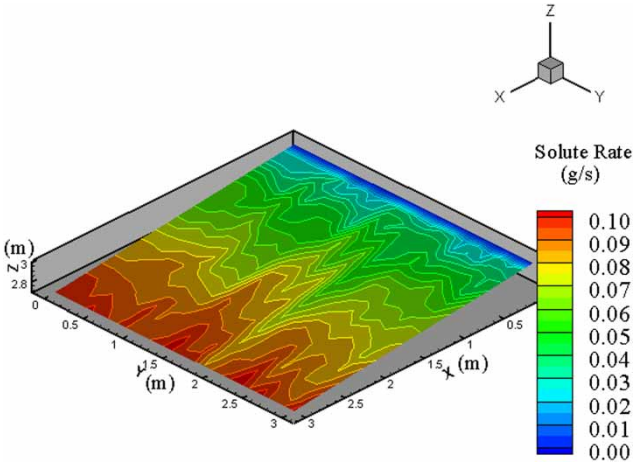

Figure 12 | Pollutant rate under the spatially varying surface roughness.

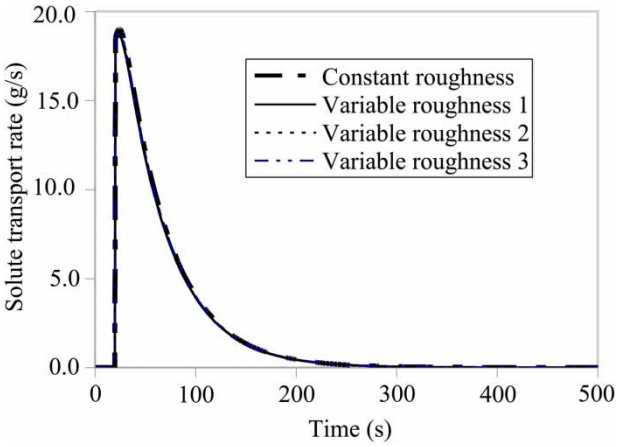

Figure 13 | Comparison of pollutant transport rate under constant (0.025) and variable surface roughness (mean is 0.025 and standard deviation is 0.009).

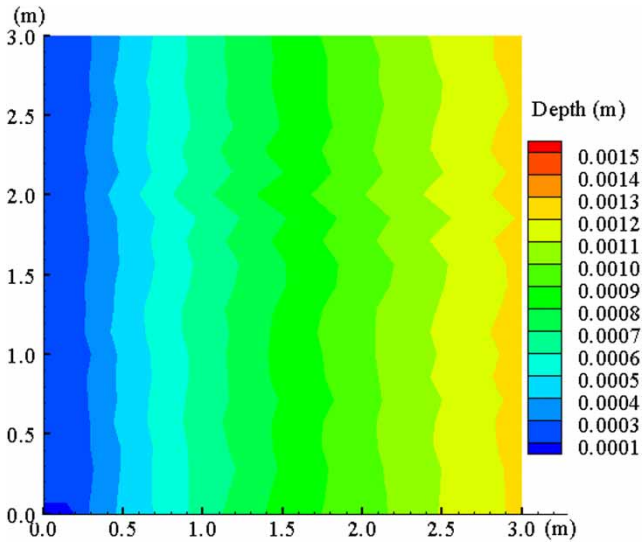

Figure 14 | Water depth under the spatially varying infiltration rate.

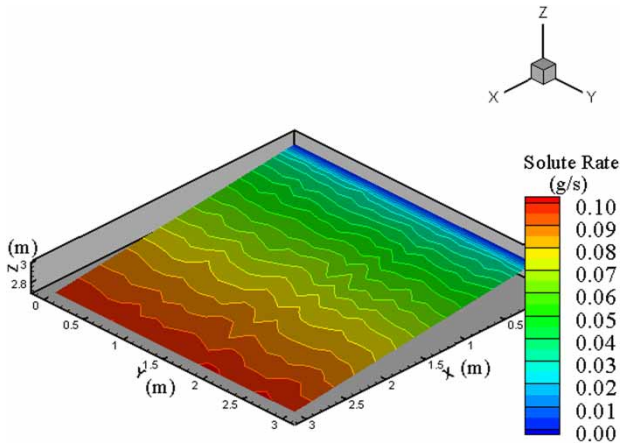

Figure 15 | Pollutant rate under the spatially varying infiltration rate.

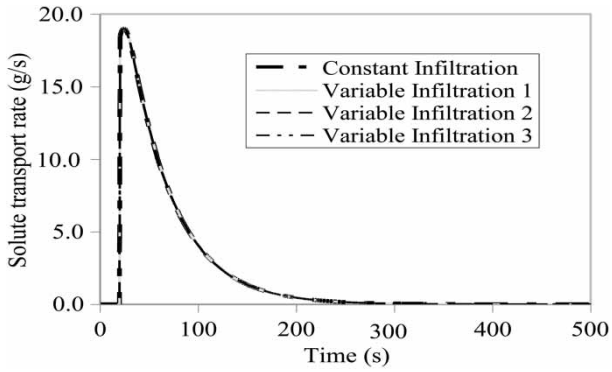

Figure 16 | Comparison of solute transport rate under constant (44 mm/h) and variable infiltration rate (mean is 44 mm/h and standard deviation is 20 mm/h).

the average infiltration rate does not influence the transport rate at the catchment outlet.

CONCLUSIONS

A two-dimensional model was developed for simulating pollutant transport in catchment sheet flow. The developed model was successfully tested against laboratory data. The effects of non-uniform characteristics of small size plot (3 m × 3 m) on pollutant transport during rainstorms were numerically investigated by the model.

The effect of varying slopes on the flow dynamics, and pollutant rates are very significant. Pollutant loads could be overestimated by about 10% if an actual spatially varying microtopography is replaced by constant average slopes. The effect of varying roughness and infiltration on pollutant transport rate at the catchment outlet is relatively negligible. Hence, the use of constant average roughness and infiltration can be justified.

The numerical tests in this study were carried out over a 3 m × 3 m small-sized plot. The results give an insight into understanding the transport process over surfaces having non-uniform characteristics. However, for realistic results, the developed model needs to be applied at a catchment scale with actual physical characteristics. The model has to be tested with field data.

ACKNOWLEDGEMENTS

This work was partially supported by the National Natural Science Foundation of China (51009120), and G. Tayfur and Z. He contributed equally to this work.

REFERENCES

Abbasi, F., Simunek, J., van Genuchten, M. T., Feyen, J., Adamsen, F. J., Hunsaker, D. J., Strelkoff, T. S. & Shouse, P. 2003 Overland water flow and solute transport: Model development and filed data analysis. *J. Irrig. Drain. Eng.* **129** (2), 71–81.

Abbott, M. B. & Refsgaard, J. C. 1996 *Distributed Hydrological Modeling*. Kluwer Academic Publisher, Dordrecht, The Netherlands.

Deng, Z.-Q., Lima, J. L. M. P. & Singh, V. P. 2005 Transport rate-based model for overland flow and solute transport: Parameter estimation and process simulation. *J. Hydrol.* **315**, 220–235.

Gitis, V. G., Petrova, E. N., Pirogov, S. A. & Yurkov, E. F. 2007 Mathematical modeling of the pollutants overland flow and transport. *Automat. Rem. Contr.* **68** (9), 1643–1653.

Govindaraju, R. S. 1996 Modeling overland flow contamination by chemicals mixed in shallow soil horizons under variable source area hydrology. *Water Resour. Res.* **32** (3), 753–758.

He, Z., Wu, W. & Wang, S. S. Y. 2009 An integrated 2D surface and 3D subsurface contaminant transport model considering soil erosion and sorption. *J. Hydraul. Eng.* **135** (12), 1028–1040.

Lima, J. L. M. P., Singh, V. P. & de Lima, M. I. P. 2003 The influence of storm movement on water erosion: Storm direction and velocity effects. *Catena* **52**, 39–56.

Peyton, R. L. & Sanders, G. 1990 Mixing in overland flow during rainfall. *J. Environ. Eng. ASCE* **116** (4), 764–784.

Stone, H. L. 1968 Iterative solution of implicit approximation of multidimensional partial differential equations. *SIAM (Soc. Ind. Appl. Math.) J. Numer. Analy.* **5**, 530–558.

Tayfur, G. & Kavvas, M. L. 1998 A really-averaged overland flow equations at hillslope scale. *Hydrol. Sci. J.* **43** (3), 361–378.

Tayfur, G. & Singh, V. P. 2004 Numerical model for sediment transport over non-planar, non-homogeneous surfaces. *J. Hydrol. Eng.-ASCE* **9** (1), 35–41.

Tayfur, G., Kavvas, M. L., Govindaraju, R. S. & Storm, D. E. 1993 Applicability of St.Venant equations for two dimensional overland flows over rough infiltrating surfaces. *J. Hydraul. Eng. ASCE* **119** (1), 51–63.

Vander Kwaak, J. E. 1999 Numerical simulation of flow and chemical transport in integrated surface-subsurface hydrologic systems. PhD dissertation, University of Waterloo, Waterloo, Ontario, Canada.

Wallach, R., Grigorin, G. & Rivlin, J. 2001 A comprehensive mathematical model for transport of soil-dissolved chemicals by overland flows. *J. Hydrol.* **247**, 85–99.

Walton, R. S., Volker, R. E., Bristow, K. L. & Smettem, K. R. J. 2000 Experimental examination of solute transport by surface runoff from low-angle slopes. *J. Hydrol.* **233**, 19–36.

Yan, M. & Kahawita, R. 2000 Modeling the fate of pollutant in overland flow. *Water Res.* **34** (13), 3335–3344.

Yan, M. & Kahawita, R. 2007 Simulating the evolution of non-point source pollutants in a shallow water environment. *Chemosphere* **67**, 879–885.

First received 23 October 2012; accepted in revised form 17 July 2013. Available online 20 August 2013

Copyright of Hydrology Research is the property of IWA Publishing and its content may not be copied or emailed to multiple sites or posted to a listserv without the copyright holder's express written permission. However, users may print, download, or email articles for individual use.